Performance Enhancement for Ultrashort-Pulse Wavelength Conversion by Using an Aperiodic Domain-Inverted Optical Superlattice

Weirui Dang, Yuping Chen, and Xianfeng Chen

***Abstract*— We propose a designed aperiodic domain-inverted optical superlattice structure, where the performance of ultrashort-pulse wavelength conversion, relative-broad and flat conversion band with high conversion efficiency, has been well-balanced and enhanced in comparison with those in periodical or linear-chirped optical superlattices. Using this structure, we present a 5.5-nm flat band with almost no pulse distortion for picosecond wavelength conversion in the C-band. Moreover, the uniformity of all inverted domains may provide more convenience for poling. The above benefits may bring promising applications in generating broadband continuous-variable entanglement source and terahertz source with equivalent generation rate.**

***Index Terms*— Nonlinear optical devices, optical frequency conversion, optical phase matching, ultrafast optics.**

I. Introduction

ULTRASHORT-PULSE wavelength converters based on quasi-phase-matched (QPM) nonlinear materials in regular domain-inverted superlattice have been demonstrated [1]-[4]. As the small wavelength and temperature tolerances limit their applications in ultrashort-pulse wavelength conversion, further progress has been focused on broadening the phase-matching bandwidth and flattening the efficiency response. We have already proposed a method of employing type I interactions [5], but the conversion efficiency was greatly decreased by the small d_{31} nonlinear coefficient. The use of a linear-chirped optical superlattice [6], [7] could offer a benefit of a large bandwidth with high conversion efficiency, but it still brings two problems: noticeable ripples on the conversion efficiency curves lead to a bad flatness response; the small chirp step in the linear-chirped optical superlattice (i.e., a few hundred picometers), leads to fabrication difficulties. Recently an efficient wideband with flat efficiency response has been numerically proposed using the step-chirped grating with fixed pumps to efficiently suppress the unwanted ripples instead of the uniform grating with detuned pumps [8]. Another technique has also proved to be useful to solve the problem by changing the duty ratio at both ends of a chirped or step-chirped grating [9], [10], or by using a deleted-reversal pattern [11]. However, the smallness of the initial inverted domain width below 2 μm scale is still a challenge to avoid the efficiency fluctuation and to put into practical applications.

To solve the fabrication difficulty as well as obtain an efficient flattop wideband, we found the aperiod optical supperlattice (AOS) grating is useful due to its uniform domain width, which has been already proposed for second harmonic interactions [12], [13]. In this letter, we propose a designed AOS grating in a MgO-doped lithium niobate waveguide (MgO:APPLN) with the uniform domain width of 3 μm, to balance and enhance the main performance of a ultrashort-pulse wavelength converter, namely the bandwidth, the conversion efficiency and the flatness response. The uniformity of the domain width avoids the small chirp step in the linear-chirped optical superlattice and provides convenience in the fabrication process.

II. Operation Principles and Numerical Design of AOS Gratings

Here, we consider cascaded sum- and difference- frequency generation (cSFG/DFG) processes for wavelength conversion. The pulsed signal (λ_S) located in C-band, generates a sum-frequency wave (λ_{SF}) and subsequent an idler (λ_i) in company with two continue wave (CW) pumps (λ_{P1}, λ_{P2}) through the cSFG/DFG processes, satisfying the QPM conditions: $1/\lambda_{SFG} = 1/\lambda_S + 1/\lambda_{P1}$, $1/\lambda_i = 1/\lambda_{SFG} - 1/\lambda_{P2}$. The evolution of these five waves can be analyzed by using a plane-wave approximation [14].

We demonstrated the MgO:APPLN waveguide of 3-cm-long via electric-field poling of a Z-cut MgO-doped lithium niobate wafer. The schematic diagram of the structure is partly shown in Fig. 1, where the sample was divided into uniform domains, for the superlattice of ferroelectrics is essentially a digitized structure with a local nonlinear coefficient $d_{eff}(x)$ that is either plus or minus that of the material. Although the smaller domain width is, the better optimal AOS grating will perform, the smallness of domain width less than 3 μm will introduce

Manuscript received August 24, 2011; revised November 12, 2011; accepted November 16, 2011. Date of publication November 29, 2011; date of current version February 10, 2012. This work was supported in part by the National Natural Science Fund of China under Grant 10874120 and Grant 11174204, and sponsored by the Scientific Research Foundation for the Returned Overseas Chinese Scholars, State Education Ministry.

The authors are with the Department of Physics, State Key Laboratory of Advanced Optical Communication System and Networks, Shanghai Jiao Tong University, Shanghai 200240, China (e-mail: ypchen@sjtu.edu.cn; xfchen@sjtu.edu.cn).

Color versions of one or more of the figures in this letter are available online at http://ieeexplore.ieee.org.

Digital Object Identifier 10.1109/LPT.2011.2177653

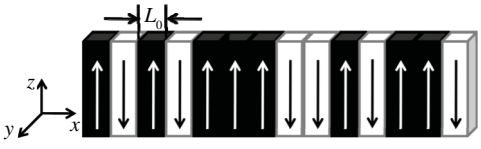

Fig. 1. Schematic diagram of MgO:APPLN in part. The black and white strips represent the positive and negative domains.

poling difficulties with aforesaid engineering methods [6]-[10] and we consequently chose $L_0 = 3\mu$m as the domain width for easing fabrication, which is less than the coherence length of 9.7 μm. The optimal domain distribution was then created by the simulated annealing (SA) method [15] by selecting appropriate objective function to achieve flat efficiency response with an arbitrary degree of band broadening. In this letter, we chose a 5.5-nm bandwidth for picosecond wavelength conversion to accord with the half-width of 1.57 ps hyperbolic-secant signal pulse spectrum for numerical simulation in Section III. Thus, the designed efficiency profile can cover the spectrum of signals, assuring that the spectrum can be equally converted to the idlers and avoiding the pulse distortion after conversion.

Figure 2 represents the efficiency profile for the designed AOS grating as well as uniform and linear-chirped gratings with the same length, where the reduced effective nonlinear coefficient d_{reff} [13], [16] divided by d_{eff} clarifies the structure effect on the efficiency response. The uniform grating period is 19.03 μm and the chirped grating period changes from 19.01 μm to 19.07 μm. The pumps are located at 1540 nm and 1535 nm to avoid occupying the 1555 nm communication channel of C-band. In Fig. 2, we can see that the uniform grating provides a quite narrow bandwidth of 0.47 nm, while the AOS grating enhances the bandwidth tenfold at the cost of peak efficiency decreased by 0.65, which provides a comparable flattop efficiency response to the linear-chirp grating, and saves the efficiencies at the edge of the conversion band so as to decrease the group velocity dispersion (GVD) effect and consequent pulse shape broadening [3]. Thus, it is possible to use the AOS grating to achieve ultrashort-pulse wavelength conversion without using any additional optical equalization. Additionally, the efficient response with pulse reshaping and amplitude modulation for ultrashort-pulse wavelength conversion can be achieved with different target conversion band by designing the objective function in the SA method.

III. Numerical Investigation and Discussion

In order to illustrate the benefit of the AOS grating in ultrashort-pulse wavelength conversion, we numerically simulated the wavelength conversion processes for picosecond pulsed signals. The cSFG/DFG interaction processes in the MgO:APPLN waveguide can be described by the coupled-wave equations [17], which can be numerically solved by using the finite difference beam propagation method (FD-BPM) [18]. The pulsed signal is assumed to be a hyperbolic-secant pulse and the two pumps are CW waves. Other parameters are addressed in Table I, where the conversion efficiency with

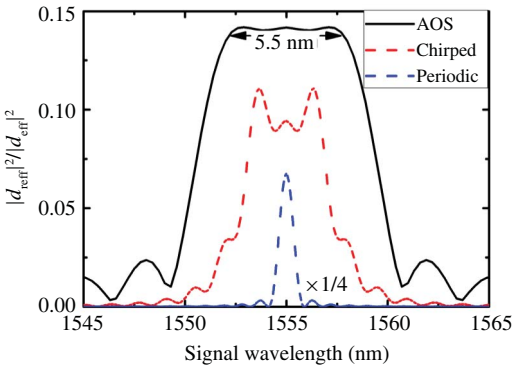

Fig. 2. Detuning from the phase-matching wavelength as a function of signal wavelength for different superlattice gratings. All the calculations are based on cSFG/DFG processes with the same device length.

TABLE I
Parameters of MgO:APPLN Waveguide [19]

Symbol	Description	Values
L	length of MgO:APPLN	3 cm
L_0	domain width	3 μm
L_c	coherence length	9.7 μm
α_S	propagation loss of each wave	0.35 dB/cm
d_{eff}	effective nonlinear coefficient	±27 pm/V
A_{eff}	effective nonlinear interaction area	50 μm^2
τ_{S0}	signal pulse width	1.57 ps
λ_S	signal wavelength	1555 nm
λ_{P1}	pump1 wavelength	1540 nm
λ_{P2}	pump2 wavelength	1535 nm
λ_i	idler wavelength	1560 nm
I_S	signal power	16.02 dBm
I_{P1}, I_{p2}	pump1 power & pump2 power	26.98 dBm
I_i	output idler power from AOS	−6.99 dBm

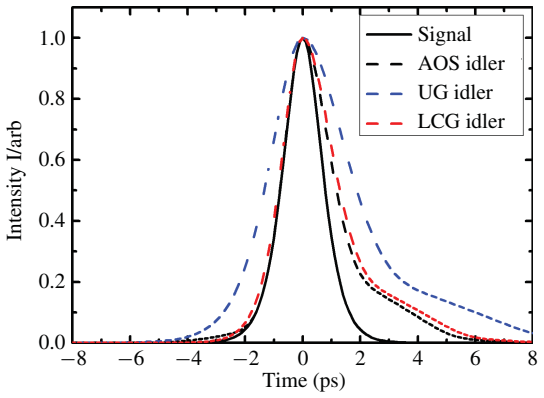

Fig. 3. Idler pulses from AOS (dashed black line), uniform (dashed blue line), and chirped (dashed red line) gratings with the same length of 3 cm. The bandwidth of idler pulses are 1.91, 3.37, and 2.21 ps, respectively.

AOS grating is calculated to be −23 dB, slightly higher than −25 dB with the chirped grating [7].

Converted idler pulses from AOS, uniform and chirped grating with the same length are presented in Fig. 3. The input signal pulsewidth was 1.57 ps, and the converted idle pulse from AOS was slightly broadened with a pulsewidth of

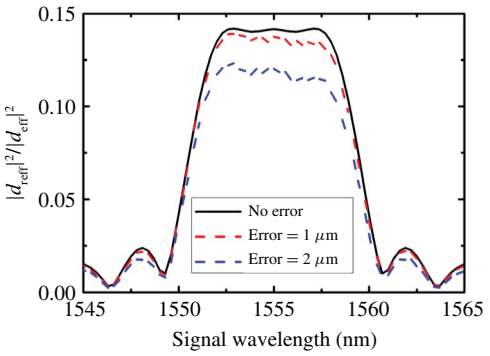

Fig. 4. Destructive effect of domain error in the efficiency profile.

1.91 ps in comparison with 2.21 ps output from chirped grating and 3.37 ps output from uniform grating. Obviously, the pulse broadening has been effectively suppressed by the designed AOS due to its good flat efficiency response and relative broad bandwidth. The caudated distortion of the idler wave is also considered due to group velocity mismatch (GVM).

For the inverted domains possibly grow beyond the width of the metal electrode under current room-temperature poling technique, the destructive effect of domain error is unavoidable. The inverted domains may extend its edge into adjacent layers with the un-inverted domains shortened, or they do not reach their pre-designed edges so that the un-inverted domains are consequently lengthened. Figure 4 indicates the destructive effect of domain error in efficiency profile and bandwidth with random domain shortening and lengthening. As the absolute domain error increases from 1 μm to 2 μm, the effective nonlinear coefficient and the quality of the broadened flattop obviously decreased from 93% to 86%. The domain error also leads to a sloping band when the bandwidth has almost no change.

IV. Conclusion

We have shown that the engineered AOS in MgO-doped lithium niobate waveguide provides a large bandwidth and a flat phase-matching response with high conversion efficiency. This technique effectively reduces the ripple in the tuning curves of the linear-chirped grating device and completely avoids the fabrication difficulty due to small chirp step or small initial width of poled region. Finally, We employed FD-BPM to help to demonstrate a cSFG/DFG interaction processes with a flattop bandwidth of 5.5 nm, which fulfills ultrashort-pulse wavelength conversions of 1.57 ps signal pulse, where the conversion bandwidth is enhanced to be tenfold wider than that of a fixed periodic grating with the same waveguide length, at the cost of peak conversion efficiency decreased only 1/3. In a wider context, the AOS technique applied in nonlinear optics is useful for generating broadband variable entanglement source [20] and THz source with equivalent generation rate.

References

[1] J. Wang, J. Q. Sun, C. H. Luo, and Q. Z. Sun, "Experimental demonstration of wavelength conversion between ps-pulses based on cascaded sum- and difference frequency generation (SFG+DFG) in $LiNbO_3$ waveguides," *Opt. Express*, vol. 13, no. 19, pp. 7405–7414, Sep. 2005.

[2] Y. Wang, J. Fonseca-Campos, C.-Q. Xu, S. Yang, E. A. Ponomarev, and X. Bao, "Picosecond-pulse wavelength conversion based on cascaded second-harmonic generation-difference frequency generation in a periodically poled lithium niobate waveguide," *Appl. Opt.*, vol. 45, no. 21, pp. 5391–5403, 2006.

[3] H. Furukawa, A. Nirmalathas, N. Wada, S. Shinada, H. Tsuboya, and T. Miyazaki, "Tunable all-optical wavelength conversion of 160-Gb/s RZ optical signals by cascaded SFG-DFG generation in PPLN waveguide," *IEEE Photon. Technol. Lett.*, vol. 19, no. 6, pp. 384–386, Mar. 15, 2007.

[4] A. Bogoni, X. Wu, I. Fazal, and A. E. Willner, "Photonic processing of 320 Gbits/s based on sum-/difference-frequency generation and pump depletion in a single PPLN waveguide," *Opt. Lett.*, vol. 34, no. 12, pp. 1825–1827, 2009.

[5] Y. Chen, F. Lu, W. Lu, and X. Chen, "Tunable all-optical wavelength conversion of a femtosecond pulse based on Cascaded $\mathcal{X}^{(2)}$ SHG + DFG interactions," *J. Korean Phys. Soc.*, vol. 55, no. 3, pp. 1282–1285, Sep. 2009.

[6] T. Suhara and H. Nishihara, "Theoretical analysis of waveguide second-harmonic generation phase matched with uniform and chirped gratings," *IEEE J. Quantum Electron.*, vol. 26, no. 7, pp. 1265–1276, Jul. 1990.

[7] G.-W. Lu, S. Shinada, H. Furukawa, N. Wada, T. Miyazaki, and H. Ito, "160-Gb/s all-optical phase-transparent wavelength conversion through cascaded SFG-DFG in a broadband linear-chirped PPLN waveguide," *Opt. Express*, vol. 18, no. 6, pp. 6064–6070, 2010.

[8] A. Tehranchi and R. Kashyap, "Flattop efficient cascaded $\mathcal{X}^{\mathrm{bm(2bm)}}$ (SFG *plus* DFG)-based wideband wavelength converters using step-chirped gratings," *IEEE J. Sel. Topics Quantum Electron.* [Online]. Available: http://ieeexplore.ieee.org, DOI: 10.1109/JSTQE.2011.2136324

[9] T. Umeki, *et al.*, "Widely tunable 3.4 μm band difference frequency generation using apodized $\mathcal{X}^{(2)}$ grating," *Opt. Lett.*, vol. 32, no. 9, pp. 1129–1131, 2007.

[10] A. Tehranchi and R. Kashyap, "Design of novel unapodized and apodized step-chirped quasi-phase matched gratings for broadband frequency converters based on second-harmonic generation," *J. Lightw. Technol.*, vol. 26, no. 3, pp. 343–349, Feb. 1, 2008.

[11] J. Huang, X. P. Xie, C. Langrock, R. V. Roussev, D. S. Hum, and M. M. Fejer, "Amplitude modulation and apodization of quasi-phase-matched interactions," *Opt. Lett.*, vol. 31, no. 5, pp. 604–606, 2006.

[12] J. Wu, T. Kondo, and R. Ito, "Optimal design for broadband quasi-phase-matched second-harmonic generation using simulated annealing," *J. Lightw. Technol.*, vol. 13, no. 3, pp. 456–460, Mar. 1995.

[13] X. Zeng, X. Chen, F. Wu, Y. Chen, Y. Xia, and Y. Chen, "Second-harmonic generation with broadened flattop bandwidth in aperiodic domain-inverted gratings," *Opt. Commun.*, vol. 204, nos. 1–6, pp. 407–411, Apr. 2002.

[14] R. W. Boyd, *Nonlinear Optics*. New York: Academic, 1992.

[15] S. Kirkpatrick, C. D. Gelatt, Jr., and M. P. Vecchi, "Optimization by simulated annealing," *Science*, vol. 220, no. 4598, pp. 671–680, May 1983.

[16] M. H. Chou, K. R. Parameswaran, and T. Taira, "Multiple-channel wavelength conversion by use of engineered quasi-phase-matching structures in $LiNbO_3$ waveguides," *Opt. Lett.*, vol. 24, no. 16, pp. 1157–1159, 1999.

[17] Y. Wang and C. Q. Xu, "Analysis of picosecond-pulse wavelength conversion based on cascaded sum-frequency generation and difference-frequency generation in quasi-phase-matched $LiNbO_3$ waveguides," *Opt. Eng.*, vol. 46, p. 055003, May 2007.

[18] J. VanRoey, J. Donk, and P. E. Lagasse, "Beam-propagation method: Analysis and assessment," *J. Opt. Soc. Amer.*, vol. 71, no. 7, pp. 803–810, 1981.

[19] J. Wang, J. Q. Sun, X. L. Zhang, and D. X. Huang, "All-optical tunable wavelength conversion with extinction ratio enhancement using periodically poled lithium niobate waveguides," *J. Lightw. Technol.*, vol. 26, no. 17, pp. 3137–3148, Sep. 1, 2008.

[20] J. S. Zhao, *et al.*, "Broadband continuous-variable entanglement source using a chirped poling nonlinear crystal," *Phys. Rev. A*, vol. 81, no. 1, pp. 013832-1–013832-5, Jan. 2010.